Copy of the:

On the efficiency of the primal–mixed finite element scheme (in 2d)

D. Mijuca and M. Berkovic, CST'98

Abstract

In the present paper a coordinate independent finite element primal–mixed approach based on the stationary Reissner's principle, having both the displacement and stress boundary conditions exactly satisfied and solvable by direct Gaussian elimination procedure, is presented. The main goal of this paper is to show that the proposed procedure is easy for implementation, robust, stable near singularities and more efficient, in the sense of the execution time needed for the prescribed accuracy, than classical displacement finite element procedure. Because Gaussian procedure is obvious in the classical finite element analysis, the proposed approach ensures a fair basis for the comparison of computational efficiencies of these two approaches.

1 Introduction

One of the most common techniques for the analysis of the deformed state of a solid body (i.e. solution of the corresponding boundary–value problems), for which exact solution cannot be found explicitly, is the finite element method. Finite element formulation of the weakly formulated boundary–value problem is obtained by seeking a critical point of the relevant funcional over a finite dimensional subspace of the admissible trial functions. The unknown fields are approximated by the set of nodal values and by interpolation functions between nodes.

An irreducible finite element scheme (e.g. the displacement procedure) is usually named a *primal finite element method*. Otherwise, if reducible, it is known as a *mixed finite element method* (it calculates simultaneously two or more variables).

Mixed finite element methods are based on formulations having also the stresses and/or strains as fundamental variables (in the mechanics of solids), at variance with the classical (primal) finite element method where fundamental unknowns are displacements only.

There are opinions [1] that mixed methods have some serious drawbacks. For instance, a fact that discrete mixed system involves more degrees of freedom than a primal one, and hence the unacceptable execution time for the *same mesh*, is considered as one of main disadvantages of mixed methods.

However, in this paper it will be shown that the present mixed model is (orders of magnitude) faster than classical finite element analysis for the *same accuracy*.

Further, the classical approach, based on an extremum principle of the minimum of the potential energy, has a positive definite system matrix. On the contrary, as a saddle point problem, mixed approach leads to an indefinite system of algebraic equations, thus narrowing the number of solution techniques that can be applied directly. Nevertheless, a usual sparse Gaussian elimination solver can be, and has been, successfully used for the solution of the resulting systems of equations of the proposed procedure.

Furthermore it has been shown, by numerical examples, that the present approach is stable near singularities, at variance with some other closely related procedures.

2 Fundamental equations and classical FE formulation

Although the classical finite element method can be applied in various mechanical problems, here we analyse finite elements of an elastic continuum.

Let us consider field equations of linear elasticity, that is the constitutive equation:

$$\mathbf{T} - \mathbf{C}:\mathbf{e}(\mathbf{u}) = \mathbf{0} \ \text{ in } \ \Omega, \tag{1}$$

and the equilibrium equation

$$div\mathbf{T} + \mathbf{f} = \mathbf{0} \ \text{ in } \ \Omega \tag{2}$$

In these expressions, $\mathbf{T}$ is the symmetric stress tensor, $\mathbf{u}$ the displacement vector, $\mathbf{e}$ denotes the infinitesimal strain tensor, $\mathbf{f}$ the vector of the body forces, $\mathbf{C}$ the elasticity tensor and Ω is an open, bounded domain of the elastic body.

In order to find out unique solution of the above equations, a traction (Neumann) and geometric (kinematic, Dirichlet) boundary conditions should be defined:

$$\mathbf{Tn} - \mathbf{p} = \mathbf{0} \ \text{ on } \ \partial\Omega_t, \tag{3}$$

$$\mathbf{u} - \mathbf{w} = \mathbf{0} \ \text{ on } \ \partial\Omega_u, \tag{4}$$

where, $\mathbf{n}$ is the unit normal vector to the (Lipschitzian) boundary $\partial\Omega$, $\mathbf{w}$ is the vector of the prescribed displacements and $\mathbf{p}$ is the vector of the boundary tractions, while $\partial\Omega_u$ and $\partial\Omega_t$ are respectively the portions of the $\partial\Omega$ where displacements and stresses are prescribed.

Weak formulation of the *primal* problem is obtained by writing the equilibrium law in weak form and integrating by parts:

Find $\mathbf{u} \in H^1(\Omega)^n$ such that $\mathbf{u}\big|_{\partial\Omega_u} = \mathbf{w}$ and

$$\int_\Omega \mathbf{e}(\mathbf{v}) : \mathsf{C} : \mathbf{e}(\mathbf{u}) d\Omega = \int_\Omega \mathbf{v} \cdot \mathbf{f}\, d\Omega + \int_{\partial\Omega_t} \mathbf{v} \cdot \mathbf{p}\, d\partial\Omega \qquad (5)$$

for all $\mathbf{v} \in H^1(\Omega)^n$ such that $\mathbf{v}\big|_{\partial\Omega_u} = 0$.

Here, $H^1(\Omega)^n$ is the space of all vectorfields which are square integrable and have square integrable gradient and n is the number of spatial dimensions of the problem under consideration, while $\mathbf{v}$ are the weight functions.

After the problem is defined in a weak form, some discretization technique should be introduced in order to find a solution over a finite dimensional space U_h of trial functions $\mathbf{u}_h$.

From the above sketch of the classical finite element displacement method (CFE) it is obvious that stresses, although often most important quantities, have to be determined *a posteriori* by differentiation in so–called post–processing part of finite element analysis which entails a loss of accuracy [1]. This is a serious drawback of the displacement finite element method and the main reason for the introduction the mixed finite element scheme as an alternative basis for studying the behaviour of continuous bodies.

3 Present primal–mixed formulation

The weak formulation of a mixed problem, associated with Hellinger–Reissner's variational principle [2] is used:

Find a pair $\{\mathbf{u}, \mathbf{T}\} \in H^1(\Omega)^n \times L^2(\Omega)^{n\times n}_{sym}$ such that $\mathbf{u}\big|_{\partial\Omega_u} = \mathbf{w}$ and:

$$\int_\Omega (\mathbf{A}\mathbf{S}:\mathbf{T} - \mathbf{S}:\nabla\mathbf{u} - \nabla\mathbf{v}:\mathbf{T}) d\Omega = -\int_\Omega \mathbf{v}\cdot\mathbf{f} d\Omega - \int_{\partial\Omega_t} \mathbf{v}\cdot\mathbf{p} d\partial\Omega \qquad (6)$$

for all $\{\mathbf{v}, \mathbf{S}\} \in H^1(\Omega)^n \times L^2(\Omega)^{n\times n}_{sym}$ such that $\mathbf{v}\big|_{\partial\Omega_u} = \mathbf{0}$.

In this expression $\mathbf{A} = \mathbf{C}^{-1}$ is the elastic compliance tensor, while $\mathbf{S}$ are test functions. Space $L(\Omega)^{n\times n}_{sym}$ is the space of all symmetric tensorfields.

Because the displacement spaces are the same as in the classical displacement approach, and the stress space can be discontinuous at the element boundaries, it is a straightforward task to construct the elements of the above type. However, it is possible to consider also the continuous stress spaces, i.e. $\mathbf{T} \in \left(H^1\right)^{n\times n}$, the space of all symmetric tensorfields that have square integrable gradient. This approach has been successfully used by Mirza and Olson [3] for linear triangles and in [4] for bilinear isoparametric quadrilaterals, and the numerical results indicated high accuracy of a model.

However, it looks that theoretical and practical aspects of the direct treatment of stress constraints as essential boundary conditions, at least in the most general case of the formulation (6), and stabilization of primal–mixed elements by *bubbles*, were first published in the papers [5,6] respectively.

3.1 Finite element subspaces

We let C_h be the partitioning of Ω into elements Ω_i and define the finite element subspaces for the displacement vector, the stress tensor and the appropriate weight functions respectively as:

$$U_h = \{\mathbf{u} \in \left(H^1\right)^n(\Omega) \Big| \mathbf{u}\big|_{\partial\Omega_u} = \mathbf{w}, \mathbf{u}\big|_{\Omega_i} = U^K(\Omega_i)\mathbf{u}_K, \forall\Omega_i \in \mathsf{C}_h\},$$

$$V_h = \{\mathbf{v} \in \left(H^1\right)^n(\Omega) \Big| \mathbf{v}\big|_{\partial\Omega_u} = \mathbf{0}, \mathbf{v}\big|_{\Omega_i} = V^M(\Omega_i)\mathbf{v}_M, \forall\Omega_i \in \mathsf{C}_h\},$$

$$T_h = \{\mathbf{T} \in \left(H^1\right)^{n\times n}(\Omega) \Big| \mathbf{T}\cdot\mathbf{n}\big|_{\partial\Omega_t} = \mathbf{p}, \mathbf{T}\big|_{\Omega_i} = T_L(\Omega_i)\mathbf{T}^L, \forall\Omega_i \in \mathsf{C}_h\},$$

$$S_h = \{\mathbf{S} \in \left(H^1\right)^{n\times n}(\Omega) \Big| \mathbf{S}\cdot\mathbf{n}\big|_{\partial\Omega_t} = \mathbf{0}, \mathbf{S}\Big|_{\partial\Omega_i} = S_L(\Omega_i)\mathbf{S}^L, \forall\Omega_i \in \mathsf{C}_h\}.$$

In these expressions $\mathbf{u}_K$ and $\mathbf{T}^L$ are the nodal values of the vector $\mathbf{u}$ and tensor $\mathbf{T}$ respectively. Accordingly, U^K and T_L are the corresponding values of the interpolation functions, connecting the displacements and stresses at an arbitrary point in Ω_i (the body of an element), and the nodal values of these quantities. The complete analogy holds for the displacement and stress variations (weight functions) $\mathbf{v}$ and $\mathbf{S}$ respectively.

3.2 Compact matrix form of the FE equations

As it has been shown in [5], problem under consideration based on (6) can be formulated in the symbolic matrix form as:

$$\begin{bmatrix} A_{vv} & -D_{vv} \\ -D_{vv}{}^T & 0 \end{bmatrix} \begin{bmatrix} t_v \\ u_v \end{bmatrix} = \begin{bmatrix} -A_{vp} & D_{vp} \\ D_{pv}{}^T & 0 \end{bmatrix} \begin{bmatrix} t_p \\ u_p \end{bmatrix} - \begin{bmatrix} 0 \\ F_p + P_p \end{bmatrix} \qquad (7)$$

In these expressions the nodal stresses $t^{L\,st}$ and displacements u_{Kq} components are consecutively ordered in the column matrices t and u respectively. The members of the matrices A and D and of the vectors (column matrices) F and P (discretized body and surface forces) are respectively:

$$A_{NuvLst} = \sum_{\mathsf{e}} \int_{\Omega_i} S_N g^a_{(N)u} g^b_{(N)v} A_{abcd} g^c_{(L)s} g^d_{(L)t} T_L \mathrm{d}\Omega, \qquad (8)$$

$$D^{Kq}_{Nuv} = \sum_{\mathsf{e}} \int_{\mathsf{E}} S_N U^K_a g^a_{(N)u} dV\, g^{(K)q}_{(N)v}, \qquad (9)$$

$$F^{Mq} = \sum_{\mathsf{e}} \int_{\Omega_i} g^{(M)q}_a V^M f^a \mathrm{d}\Omega, \qquad (10)$$

$$P^{Mq} = \sum_{\mathsf{e}} \int_{\partial\Omega_{it}} g^{(M)q}_a V^M p^a \mathrm{d}\partial\Omega, \qquad (11)$$

where

$$g^{(K)m}_{(L)s} = \delta_{kl} g^{(K)mn} \frac{\partial z^k}{\partial x^{(K)n}} \frac{\partial z^l}{\partial y^{(L)s}}, \qquad (12)$$

$$g^a_{(L)s} = \delta_{kl} g^{ab} \frac{\partial z^k}{\partial \xi^b} \frac{\partial z^l}{\partial y^{(L)s}}, \qquad (13)$$

$$g^{(K)q}_b = \delta_{kl} g^{(K)qp} \frac{\partial z^k}{\partial \xi^b} \frac{\partial z^l}{\partial x^{(K)p}}. \qquad (14)$$

are the Euclidean shifters. In these expressions z^i (i, j,k,l=

1,2,3) are the global Cartesian coordinates, while $x^{(K)n}$ (m,n,p,q =1,2,3) and $y^{(L)s}$ (r,s,t,u,v=1,2,3) are local (nodal) coordinates, used for determination of the nodal displacements and stresses respectively. Commonly used notions, $\xi^a\,(a,b,c,d=1,2,3)$ are taken for the local (element) coordinates, usually convected (parametric, isoparametric). Further, $g^{(K)mn}$ and g^{ab} are the components of the contravariant fundamental metric tensors, the first one with respect to $x^{(K)n}$ and the second to ξ^b. Computation of these quantities is described in detail per instance in [6]. Furthermore, $U_a^K = \partial U^K / \partial \xi^a$. Finally, A_{abcd} are the components of the elastic compliance tensor A, while f^a and p^a are the body forces and boundary tractions, respectively. Integration is performed over the domain Ω_i of each element, or over the part of the boundary surface $\partial\Omega_{it}$ where the tractions are given, while summation is over all the e elements of a system.

Because the tensorial character [7] of (6) is fully respected, one can choose at each global node different coordinate systems for the stresses and/or displacements, for the most convenient application of boundary conditions and interpretation of output results.

3.3 Solvability of a system

When solvability and stability of a solution of (7) are considered, LBB (Ladyzhenskaya, Babuska, Brezzi) condition [8] is often cited. Here some of its algebraic implications will be elaborated. In the accordance with Carey and Oden [9] p. 134, if LBB is to hold, we should have

$$\dim T_h \geq \dim \nabla U_h \tag{15}$$

In the present context

$$\nabla U_h = \{2\mathbf{e}_h = \nabla \mathbf{u}_h + \nabla \mathbf{u}_h^t,\ \mathbf{u}_h \in U_h\}, \tag{16}$$

is evidently a *strain* subspace. Let us discuss now the dimensions (number of entries) of the finite element spaces under consideration. In the absence of the boundary conditions, and if the same mesh is used for both the displacements and stresses, taking also into account the symmetry of the stress tensor, the dimensions of the displacement, strain and stress spaces will be respectively:

$$\begin{aligned} &n_u = \dim U_h = n\,N_u;\quad n_t = \dim T_h = \tfrac{1}{2}n(n+1)N_t;\\ &n_e = \dim \nabla U_h = \tfrac{1}{2}n(n+1)N_u. \end{aligned} \tag{17}$$

Certainly, T_h and ∇U_h are the spaces of the second order tensors. Each of these tensors has $n(n+1)/2$ components, where n is the number of spatial dimensions of the problem under consideration. Furthermore, N_t is the number of nodes of a *stress mesh*, while N_u is the number of nodes of a *displacement mesh*. From (15) and (16) it follows directly that, in the absence of the stress boundary conditions, (15) will be satisfied if

$$N_t \geq N_u. \tag{18}$$

This relationship justifies the relative success of the scheme [2,3,4,23], where $N_t \equiv N_u$.

If (some or all) of the stress boundary conditions are enforced, the number of unknown nodal stresses in (7) is decreased. Hence, the conditions (15) and consequently (18) are endangered. In practice, this means that the solution of (7) is likely to fail. To eliminate the problem one can apply, instead of (18), a somewhat conservative heuristic rule

$$N_t - N_t^* \geq N_u. \tag{19}$$

In this expression, N_t^* is the number of nodes having at least one of the stress components prescribed. It is evident that (19) cannot be satisfied for $N_t = N_u$ i.e. if the same mesh is used for both the displacements and stresses. Hence it is necessary to enrich the stress mesh by the additional nodes. Note that, due to Arnold [1], enrichment of the space $\mathbf{T}_h$ increases stability of a solution. More details will be given in the discussion on the numerical example.

3.4 Some details of the solution procedure

For the sake of the better insight in the solution procedure, the two-dimensional model problem will be considered. In that case for the each mutually interconnected (by the common element(s)) pair of nodes L and M, or L and K, respectively, submatrices of A and D have following structure:

$$A_{LM} = \begin{bmatrix} A_{L11M11} & 2A_{L11M12} & A_{L11M22} \\ A_{L12M11} + A_{L21M11} & 2A_{L12M21} + 2A_{L21M12} & A_{L12M22} + A_{L21M22} \\ A_{L22M11} & 2A_{L22M12} & A_{L22M22} \end{bmatrix} \tag{20}$$

$$\left[D_{Lst}^{Kq}\right] = \begin{bmatrix} D_{L11}^{K1} & D_{L11}^{K2} \\ D_{L12}^{K1} + D_{L21}^{K1} & D_{L12}^{K2} + D_{L21}^{K2} \\ D_{L22}^{K1} & D_{L22}^{K2} \end{bmatrix} \tag{21}$$

In these expressions indices 1 and 2 correspond to the displacements at the node K, while the indices 11, 12, 21 and 22 correspond to the stresses at nodes L and/or M.

The first main programming step in the above problem is an assembly procedure of the left and right sides of (7). The second one is the solution procedure of the resulting system (7). The most natural and fastest way in the assembly procedure of (20) and (21) is to loop through the elements with putting in connection pairs of nodes L and M. At the left side of (20) the unconstrained degrees of freedom (components t_v and u_v) connected with the current node L are retained. At the right side the terms connected with the known components t_p and u_p) are situated. The rows and columns connected with the components with zero t_p and u_p are neglected.

It should be noted also that the assembly procedure has been performed using the loops over the tensorial indices in the expressions for (8)–(11), which looks to be more efficient than matrix formulation. The matrix on the left side of (7) is indefinite, but it is also symmetric and sparse.

Consequently, the symmetric sparse Gaussian elimination procedure can be used for the solution. Zeroes at the main diagonal of the system matrix are not an obstacle because triangularization procedure fills these positions with nonzero values.

It has been shown by the numerical examples that, despite the fact that the resulting system (7) is obviously larger than in the classical finite element analysis, the efficiency of the procedure, measured as the accuracy versus the solution time, is in favour of the mixed formulation.

3.5 On the construction of stable elements and efficient solution procedure

The question of stability of the present scheme, as of a saddle–point problem, is of paramount importance. For the purpose of forming the stable primal–mixed system of algebraic equations, the results of the section 3.3 were taken into account. If there are no traction boundary conditions, the same bilinear shape functions for displacements and stresses are sufficient to maintain the solvability of a system, see (18). On the other hand, when essential traction boundary conditions are introduced, number N_t has to be increased (at least by a central, *bubble* node or by all additional five quadratic nodes, not necessarily in all elements) to satisfy (19).

Further, an efficient solution procedure is obtained by reordering of nodes in that way that degrees of freedom connected with additional nodes always appear first in the solution procedure. Note that this is nothing else than a *nested dissection* [16] ordering.

4 Numerical examples

In order to illustrate the efficiency of the present primal–mixed finite element method two–dimensional plane stress linear isotropic elastic model problems were examined.

The present procedure has been compared with the classical displacement type procedure (CFE) based on a primal scheme. In the case of the displacement procedure calculations of stresses were done *a posteriori* (in so called post–processing part of finite element analysis) either with local stress smoothing by averaging the stresses at global nodes (CFEavrg) or by the global projection procedure (FEDSS) [10].

The strain energy U_h of finite element solution is given by:

$$U_h = \frac{1}{2} \sum_{\mathsf{e}} \int_{\Omega_i} \mathbf{T}_h : \mathbf{A} : \mathbf{T}_h \, \mathrm{d}\Omega_i \tag{22}$$

where $\mathbf{T}_h$ is finite element stress. The popularity of this measure is partially due to a fact that it is, at a system level, equal to the work of the external forces W (at least for hyperelastic materials) which can be easily calculated [12].

For the energy error determination in this paper we will use the expressions of the type

$$\eta = \frac{\left| 2U - 2U_h \right|}{\left| 2U \right|} \cdot 100\% \tag{23}$$

representing *relative percentage error* [13] or *precision* [14], where U is the exact or estimated strain energy.

Let's now explain the notion of different suffixes added to the present method acronym FEMIX. If the primal–mixed scheme has the suffix BL, this means that same spaces for both fields of interest (here displacement and stresses) are chosen and that there is no traction boundary conditions introduced. Further, suffix HB indicates that stress mesh is enriched with additional bubble nodes in all elements. Finally, if there is a suffix HBB, stress *bubble* nodes are added only in elements along a physical boundary.

It is known that at each finite element mesh global node there are as many degrees of freedom as there are components of, for example, displacement vector and stress tensor. In the present paper a zero value (0) denotes the constrained degree of freedom (i.e. homogeneous boundary conditions – zero boundary condition), while value 1 denotes an active degree of freedom. Finally, value 2 denotes the prescribed component given as an input value (non–homogeneous boundary condition – arbitrary boundary condition). For example, in the case of a planar stress state (two–dimensional coordinate system), the degrees of freedom at node A can be completely determined as A20101. First three digits represent the degrees of freedom corresponding to the stresses t^{11}, t^{12} and t^{22} respectively. Similarly, fourth and fifth digit represent the degrees of freedom corresponding to the displacements u_1 and u_2.

4.1 The square plate with a circular hole

A problem of the square plate with a circular hole [15] is depicted in Figure 1. Only a quarter of it, or in the case of the present FEMIX scheme one eighth, is analyzed due to the symmetry of that system. Isotropic, homogeneous material properties and the plane stress behavior are assumed. Modulus of elasticity and Poisson's coefficient have been taken to be E=1 and ν=0.3. Plain isoparametric four-noded quadrilateral elements and 2×2 or 3×3 Gauss quadrature are used.

To get an idea about the stress and displacement behavior, the stress value $\mathsf{t} = t^{xx}$ at the point C is recorded, which is positive and hence equals the supreme norm (because of the extremal value of the stress at that point), and the largest displacement value $\mathsf{u} = u_x$ at a point B. Converged values of these stress and displacement, found by extrapolation, are approximately t=10.364 and u=6.4358. The first value is slightly at variance with the reference one [15] t=10.385.

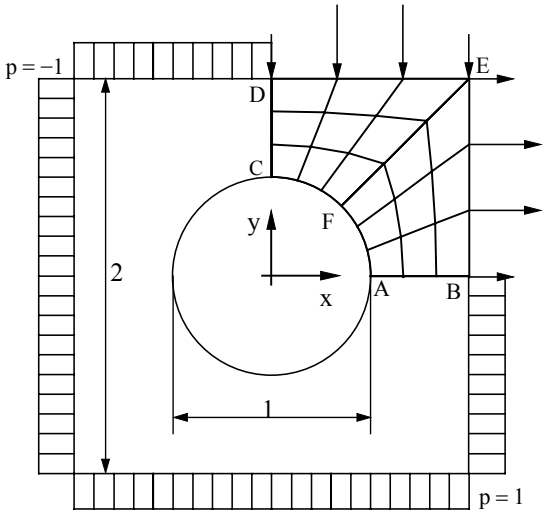

Figure 1: *Plate with a circular hole*

The numerical studies were made for the sequence of meshes having 1, 2, 4, 8, 16, 20, 32, 36, 44 and 48 elements along the side AB. The maximum norm of displacement field u occurring at the node B and maximum norm of stress field t (stress concentration) occurring at node A, were examined. Work of external forces W and strain energy of recovered stresses by simple stress averaging at global finite element nodes U(CFEavrg) were also considered.

Classical FE analysis (CFE) results are given in the Table 1:

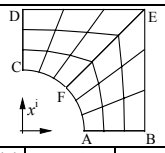

Plate with a hole
Classical *displacement* FE method
(primal scheme)

model	u(B)	t(A) via Hookean law	W	U_h(CFEavrg)	exec.time (s)
1	3.90504	5.77385	2.38977	3.298750	3.90
2	5.03788	7.68704	2.90206	3.067867	4.45
4	5.93315	9.72333	3.33323	3.261839	6.48
8	6.29405	10.4020	3.51169	3.439040	16.70
16	6.39913	10.4841	3.56434	3.534200	85.52
20	6.41223	10.4768	3.57092	3.549730	156.81
24	6.41939	10.4673	3.57453	3.558870	286.55
32	6.42655	10.4506	3.57813	3.568618	858.49
36	6.42848	10.4434	3.57910	3.571396	1403.29
38	6.42923	10.4403	3.57948	3.572488	1759.21

Table 1: Plate with a hole – displacement method

Raw stresses (CFEraw) at global nodes are calculated by the use of the Hookean law and smoothed by simple stress averaging afterwards (CFEavrg). In the next Table 2 the present FEMIX HB method results are given:

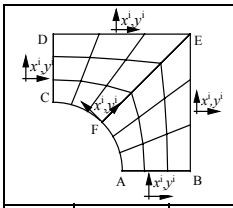

AB [10110] A [00110]
BE [20111] B [20110]
CD [10101] C [00101]
DE [10211] D [10201]
AC [00111] E [20211]

Plate with a hole
primal–mixed scheme
FEMIX HB
bubble nodes in all elements

model	u(B)	t(A)	U_h	ndof	exec. time (s)
1	5.800648	8.098980	3.118819	19	3.25
2	6.322119	7.798996	3.393532	70	4.72
4	6.479586	9.699640	3.540084	268	13.57
8	6.453713	10.18201	3.573937	1048	73.38
16	6.440977	10.31413	3.580788	4144	651.36
20	6.439182	10.33147	3.581529	6460	1602.84
24	6.438176	10.34117	3.581922	9288	3403.40

Table 2: Plate with a hole – present method FEMIX HB

In the present implementation of the proposed primal–mixed scheme it is possible to define homogeneous and non–homogeneous boundary conditions in arbitrary coordinate systems. Therefore, also one–eighth of starting model problem has been considered and obtained numerical results are given in the Table 3:

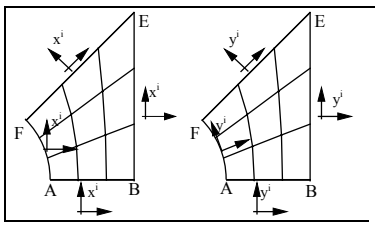

AB [10110]
EF [01001]
AF [00111]
BE [20111]
A [00110]
B [20110]
F [00001]
E [02001]

Plate with a hole
primal–mixed scheme
FEMIX HB
method
bubble nodes in all elements

model	u(B)	t(A)	U_h	ndof	exec. time (s)
1	5.80065	8.09898	3.118819	9	3.30
2	6.32212	7.79810	3.393532	34	3.74
4	6.47959	9.69964	3.540084	132	6.71
8	6.45371	10.1820	3.573937	520	31.36
16	6.44098	10.3141	3.580788	2064	201.30
20	6.43918	10.3315	3.581529	3220	422.09
24	6.43818	10.3412	3.581922	4632	836.13
32	6.43715	10.3511	3.582304	8224	2720.57
36	6.43687	10.3538	3.582406	10404	4558.44
38	6.43676	10.3549	3.582444	11590	5769.16

Table 3: Plate with a hole – present method FEMIX HB

In Figure 2 relative strain energy error norms (relative percentage error) related to the number of elements along side AB are shown.

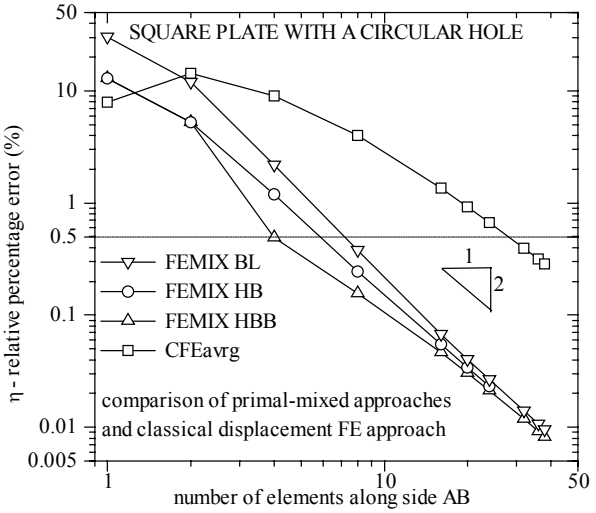

Figure 2: Percentage error versus number of elements

Further, in Figure 3 relative strain energy error norms related to the time of execution are compared.

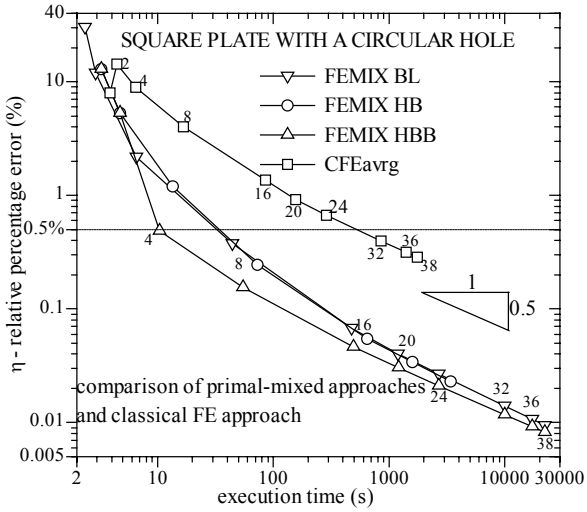

Figure 3: Percentage error versus execution time

From the Figure 3 it can be concluded that the case with the stress *bubble* nodes located only in elements along a physical boundary (HBB) is more efficient over the case when we have bubble nodes in all elements (HB), and also over the simple bilinear approach (BL) without boundary tractions

conditions applied. Anyhow, all these approaches are clearly superior compared with the classical analysis (CFE), irrespectively on the method of postprocessing used in that procedure.

4.2 Uniformly loaded ring

For the purpose of the comparison of present formulation with some analytical solutions, a problem of a thin uniformly loaded ring (Lamé, 1852) by the internal pressure of 10 units, shown in Figure 4, is considered. The internal diameter of a ring has 5 and the external one 20 units. Material characteristics are given by the Young modulus E=1 and Poisson's ratio ν=0.3. The thickness of the ring is 1. Exact value of strain energy is $U = 1.791666\overline{6}\int_{\theta} d\theta$, and for θ=π/2 strain energy has the value U=2.814343, where angle θ is angle between the side AB and CD. Circular stress is positive and its maximum value is on the internal contour, $t_{\theta\theta} = 11.333333\overline{3}$.

By taking advantage of symmetry of the model and in the case of the present primal–mixed scheme possibility of defining homogeneous and non–homogeneous boundary conditions in arbitrary coordinate systems, only one row of elements is considered. Hence, for model with n elements, inner angle has value $\theta = (\pi/2)/n$.

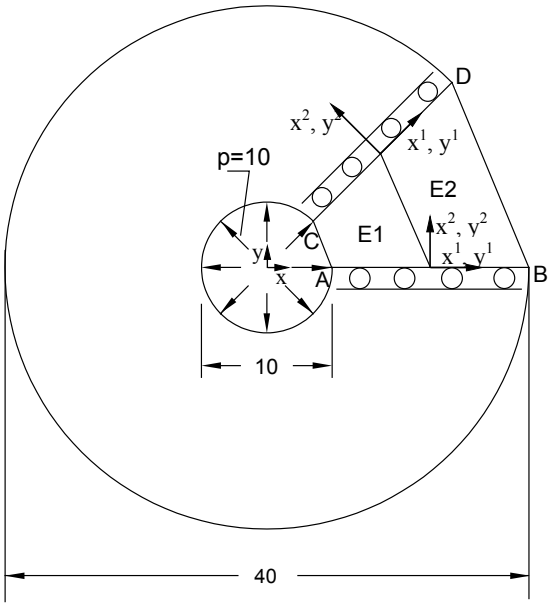

Figure 4: Uniformly loaded ring – model problem

Finite element models with 2^n elements are examined, where n=0,1,2,3,4,5,6,7,8,9,10. Because only one row of elements is considered the mesh with 2^{10}=1024 elements is equivalent to the complete (circular) model with 4×1024×1024=4,194,304 elements, or more than 20 million DOF (degrees of freedom). Hence, this model is a convenient example to give an impression about the number of significant digits obtainable by the use of very fine meshes, see Table 4–5.

Uniformly loaded ring – primal mixed method FEMIX HB

model	t_{11}(A)	strain energy U	ndof	time(s)
0	.11533226828E+02	.27836385592E+01	11	3.57
1	.97551695546E+01	.25721519285E+01	20	3.79
2	.10351126161E+02	.26934190217E+01	38	4.06
3	.10946698017E+02	.27729614576E+01	74	4.89
4	.11210658629E+02	.28023889704E+01	146	6.43
5	.11298567195E+02	.28111419026E+01	290	12.74
6	.11324057751E+02	.28135156219E+01	578	27.90
7	.11330936082E+02	.28141329872E+01	1154	58.65
8	.11332723859E+02	.28142903721E+01	2306	134.62
9	.11333179671E+02	.28143301021E+01	4610	344.93
10	.11333294754E+02	.28143400827E+01	9218	1060.11

Table 4: Uniformly loaded ring – numerical results

Uniformly loaded ring – primal mixed method FEMIX HB2				
model	t_{11}(A)	strain energy U	ndof	time(s)
0	.11533226828E+02	.27836385592E+01	11	3.74
1	.97702310751E+01	.25845676760E+01	17	3.51
2	.10383755373E+02	.26979634531E+01	32	3.78
3	.10957248858E+02	.27743799377E+01	62	4.23
4	.11212468965E+02	.28026598207E+01	122	5.38
5	.11298764167E+02	.28111826333E+01	242	8.95
6	.11324063066E+02	.28135212168E+01	482	23.34
7	.11330931096E+02	.28141337244E+01	962	47.73
8	.11332721767E+02	.28142904669E+01	1922	102.28
9	.11333179038E+02	.28143301141E+01	3842	255.79
10	.11333294582E+02	.28143400843E+01	7682	786.81

Table 5: Uniformly loaded ring – numerical results

In the Figure 5 the influence of different type of node ordering in FE mesh is shown. *Ordinary* means that sequential ordering on side AB, and then on side CD, is applied. Once again superiority of so–called *nested disection* ordering of nodes is shown. Efficiencies of present method with different stress approximations are shown in Figure 6. By FEMIX HB2 approach where stress *bubble* nodes are activated only in odd elements (E1, E3,..., see Figure 4), is denoted. If all additional five *hierarchical* local nodes are active this approach is denoted as FEMIX H.

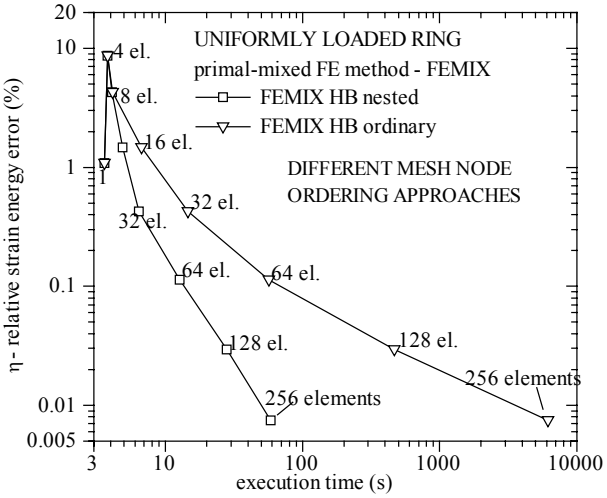

Figure 5: Efficiency as a function of node node ordering

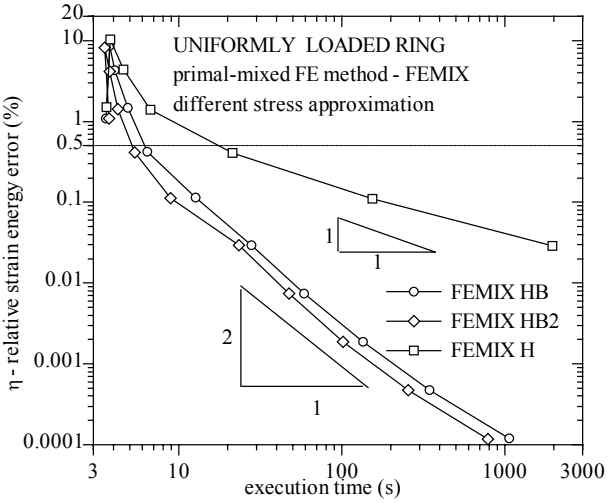

Figure 6: Efficiencies of the present approaches

The stress convergence at the supreme stress node A versus to number of elements is shown in the Figure 7. The convergence is monotonic, except between the meshes for n=0 and n=1

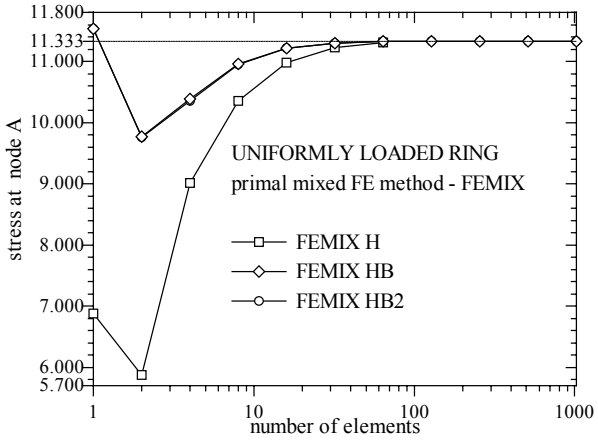

Figure 7: Uniformly loaded ring stress convergence at A

4.3 Cook's membrane problem

A well known Cook's membrane problem [17] is shown in the Figure 8.

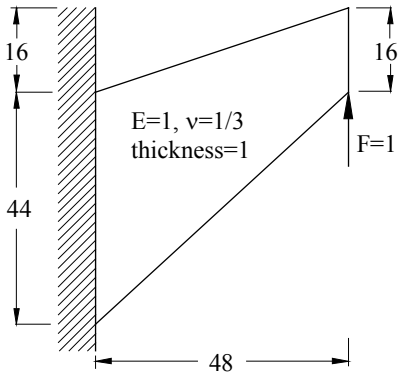

Figure 8: Cook's membrane problem

In the next Figure 9 a typical nonrectangular finite element mesh and coordinate systems, global z^i, displacement x^i and stress y^i coordinate systems together with degrees of freedom description at global nodes are shown.

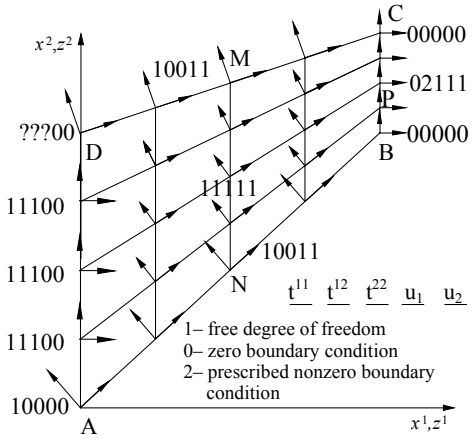

Figure 9: Defining of degrees of freedom

It should be noted that coordinate systems at stress *bubble* nodes, although can be arbitrary are taken to be Cartesian and parallel to the global frame of reference. Further, orientations of the stress coordinate systems at interior nodes are deliberately chosen as shown.

In the Table 6 numerical results for the strain energy of the raw stresses U(CFEraw), strain energy of the smoothed solution U(CFEavrg), vertical displacements u_y(P) at node P(48,52) and stress t_{11} at node M(24,52) (converged values expected to be 23.96 and -.2035 respectively) [18] and execution time (PC486/133MHz) for the displacement method, solved by the same Gaussian elimination solver as present method, are given.

displacement method CFE and local stress averaging CFEavrg Cook's membrane problem						
model	t_{11}(M)	u_y(P)	E(CFEaraw)	E(CFEavrg)	ndof	time(s)
2×2	-.4153481E-01	.119137E+02	.592374E+01	.375724E+01	27	1.92
4×4	-.1180536E+00	.183594E+02	.915311E+01	.673760E+01	75	3.68
8×8	-.1691771E+00	.221201E+02	.110420E+02	.983369E+01	243	8.50
16×16	-.1913339E+00	.234557E+02	.117282E+02	.113137E+02	867	30.87
32×32	-.1989706E+00	.238314E+02	.119345E+02	.118064E+02	3267	152.03

Table 6: displacement method – Cook's model

Numerical results obtained with the present primal–mixed FEMIX HB approach are given in the Table 7:

primal–mixed scheme FEMIX HB Cook's membrane problem					
model	t_{11}(M)	u_y(P)	W	ndof	time(s)
2×2	-.200672E+00	.228086E+02	.112718E+02	35	2.75
4×4	-.195326E+00	.235222E+02	.117886E+02	135	5.16
8×8	-.201875E+00	.239231E+02	.119698E+02	527	23.01
16×16	-.203007E+00	.239753E+02	.120053E+02	2079	111.55
32×32	-.203333E+00	.239758E+02	.120150E+02	8255	1367.16

Table 7: primal–mixed method – Cook's model

Present model problem is also interesting because there is a stress singularity at the point D. The behaviour of the normal stress component, parallel to the edge CD, for the mesh 32×32 is shown in Figure 10. Note that the stress behaviour near singularity, which is somewhat unstable for FEMIX BL scheme, is stabilized by the use of FEMIX HB

scheme. Note that, the stress boundary conditions for the model HB are enforced at each node except D.

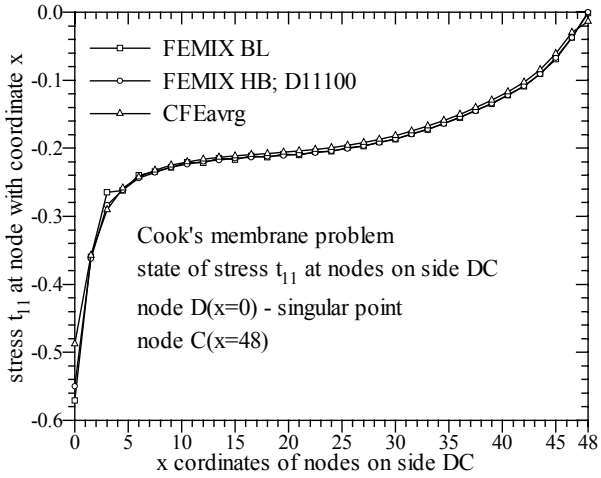

Figure 10: Cook's problem stress state along the side DC

5 Conclusions

In the present paper a solution procedure of the primal–mixed finite element equations based on the Reissner's principle has been presented. On the basis of the above analysis and the numerical results one can conclude, first, that the mixed elements with complete continuity can be practically realized, second, that simple and clear measures for the enhancement of the stability of a solution of the resulting equations are available, and finally, that the present mixed procedure is about *two orders of magnitude* more efficient than the classical finite element analysis

References

[1] D.N. Arnold, "*Mixed finite element methods for elliptic problems"*, Comput. Methods Appl.. Mech. Engrg., vol 82, 281-300, (1990)

[2] O.C. Zienkiewicz and R.L. Taylor, "*The Finite Element Method*, VOL I", McGraw- Hill, London, (1989)

[3] F.A. Mirza and M.D. Olson, "*The mixed finite element in plane elasticity*", IJNM in engineering, vol 15, 273-289, (1980)

[4] M. Berkoviæ and Z. Draškoviæ, "*Stress continuity in the finite element analysis*", in J. Robinson, ed., Accuracy, Reliability and Training in FEM Technology, Robinson and Associates, (1984)

[5] M. Berkoviæ and Z. Draškoviæ, *"On the essential mechanical boundary conditions in two-field finite element approximations"*, Comput. Methods Appl. Mech. Engrg., vol 91, 1339-1355, (1991)

[6] M. Berkoviæ and Z.V. Draškoviæ, *"A two-field finite element model related to the Reissner's principle"*, Theoretical and Applied Mechanics, vol 20, 17-36, (1994)

[7] Z. Draškoviæ, "*On invariance of finite element approximations*", Mechanika Teoretyczna i Stosowana, vol 26, 597–601 (1988)

[8] F. Brezzi and M. Fortin, *"Mixed and Hybrid Finite Element Methods"*, Springer-Verlag, New York, (1991)

[9] G. Carey and J.T. Oden, "*Finite Elements: A Second Course*", Prentice-Hall, Englewood Cliffs, (1983)

[10] D. Mijuca, Z. Draškoviæ and M. Berkoviæ, "*Displacement Based Stress Recovery Procedure*", Advances in Finite Element Technology, Civil-Comp Press, 127–134, (1996)

[11] M.D. Olson, "*The mixed finite element method in elasticity and elastic contact problems*", in S.N. Atluri, R.H.Gallagher and O.C.Zienkiewicz, eds., Hybrid and Mixed Finite Element Methods, John Wiley & Sons, 19–49,(1983)

[12] G. Strang and G.J. Fix, "*An analysis of the finite element method*", Prentice Hall, Englewood Cliffs, N.J., (1973)

[13] O.C. Zienkiewicz, J.Z.Zhu, "*A simple error estimator and adaptive procedure for practical engineering analysis*", IJNM in engineering, vol 24, 337–357, (1987)

[14] P. Becker and H.G. Zhong,"Mesh adaption for two dimensional stress analysis", Advances in Post and Preprocessing for Finite Element Technology, Civil-Comp Press, 47–59, (1994)

[15] A.K Rao, I.S. Raju and A.V. Krishna Murty, "*A powerful hybrid method in finite element analysis*", IJNM in engineering, vol 3, 389–403, (1971)

[16] O. Axelsson and V.A. Barker, "*Finite element solution of boundary value problem*", Accademic Press, Inc, (1984)

[17] R. Cook, "*Improved two–dimensional finite element*", Journal of the Structural Division, 851–1863, (1974)

[18] A.A. Canarozzi, M. Canarozzi, "*A displacement scheme with drilling degrees of freedom for plane elements*", IJNM in engineering, vol 38, 3433–3452, (1995)

[19] J. T. Oden and H. J. Brauchli , "*On the calculation of consistent stress distributions in finite element approximations*", IJNM in engineering, vol 3, 317–325, (1971)

[20] G. Cantin, G. Loubignac, and G. Touzot, An iterative algorithm to build continuous stress and displacement solutions, IJNM in engineering, vol 12, 1493-1506, (1978)

[21] J.H. Argyris, Th.L. Johnsen and H.-P. Mlejnek, "*On the natural factor in nonlinear analysis*", Comput. Methods Appl. Mech. Engrg., vol 15, 365-388, (1978)

[22] M. Berkovi} and Z. Dra{kovi}, "*An efficient solution procedure in mixed finite element analysis*", in NUMETA 85, J. Middleton and G.N.Pande, eds., (Balkema , Rotterdam, , 625-633, (1985)

[23] M. Berkoviæ, Z. Draškoviæ and D. Mijuca, *"A direct block sparse solution of the mixed finite element equations"*, Computer Assisted Mechanics and Engineering Sciences, vol 5, 21–30. (1998)